Design of a PXR experiment based on the NCEL *

XIANG Xin-Lei(相新蕾)[1,2;1)] LUO Xiao-Wei(罗小为)[3,1] XIE Jia-Lin(谢家麟)[1]
PEI Guo-Xi(裴国玺)[1] XIE Ya-Ning(谢亚宁)[1]

[1] Institute of High Energy Physics, Chinese Academy of Sciences, Beijing 100049, China
[2] Graduate University of Chinese Academy of Sciences, Beijing 100049, China
[3] University of Science and Technology of China, Hefei 230026, China

Abstract Parametric X-ray Radiation (PXR) can be used as a novel, quasi-monochromatic energy-tunable and high-yield X-ray source. It is produced at the Bragg angle by a relativistic electron beam passing through the periodic structure of crystal materials. This article concerns the PXR experiment using low energy electrons (10 MeV) from NCEL (Novel Compact Electron-Linac). The difficulty of the experiment is to distinguish the PXR photons form the background. The design of the experiment relies mainly on the yield of PXR, the Bremsstrahlung background of the X-rays and the capability of the detector.

Key words Parametric X-ray Radiation (PXR), Novel Compact Electron-Linac (NCEL), Bragg angle

PACS 41.50.+h, 41.75.Fr

1 Introduction

Parametric X-ray Radiation (PXR) is produced at the Bragg angle by a relativistic electron beam passing through the periodic structure of crystal materials. The pseudophoton theory can completely explain the PXR mechanism [1]: if a relativistic electron is moving ahead, the electromagnetic field around the electron can be described as a cloud of "virtual photons" covering a broad range of energies. These virtual photons diffract from the crystallographic planes according Bragg's law. So the X-ray produced at the Bragg angle is intense, monochromatic and highly-oriented. The energy of the PXR is related to the d-spacing of the crystal and the diffraction angle. Therefore the PXR is energy-tunable through changing the diffraction angle and the crystal. Because of these attractive features, the PXR can be used as a novel, quasi-monochromatic energy-tunable and high-yield X-ray source in medical diagnostic imaging, material science and so on.

The theory is confirmed by several experiments using high energy electron beams [2–4] (above 30 MeV). In this article we will be concerned with low energy electrons (10 MeV) from the NCEL (the Novel Compact Electron-Linac). The NCEL works without the Triode Gun, whose function is substituted by a special high power klystron. The cathode of the klystron produces electrons with pulse lengths of 7 μs and a beam energy of 120 keV, which first magnify the microwave (similar to be the common klystrons, and are then injected into the accelerating tube after energy modulation and phase modulation. After acceleration the energy of the beam is about 10 MeV and the current of the beam in a pulse of up to 100 mA in magnitude can be controlled by a diaphragm.

The difficulty of the experiment is to distinguish the PXR photons from the background which includes the dispersion of electrons, Bremsstrahlung, Transition radiation and Cerenkov radiation. The decisive part of this experiment is to control the magnitude of the background such that it is less than the yield of the PXR.

The design of the experiment relies mainly on the production of the PXR, the background of the X-rays and the capability of the detector. The detector of the experiment is a 500 μm Si Amptek XR-100 detector the dead time of (fast channel) 400 ns.

2 Energy and yield of the PXR

The energy of the PXR depends on the d-spacing

Received 22 July 2009, Revised 28 September 2009
* Supported by National Natural Science Foundation of China (10555001)
1) E-mail: xiangxl@ihep.ac.cn

between the crystal planes and the diffraction angle. It almost does not depend on the energy of the electron. The PXR energy is given by [5]

$$E_n = n\frac{hc}{d}\frac{\beta\sin\theta_{\rm B}}{1-\sqrt{\varepsilon}\,\cos\theta_{\rm D}},$$

where E_n is the photon energy, n is the diffraction order, d is the interplanar spacing, $\theta_{\rm B}$ is the angle between the crystal plane and the particle momentum (Bragg angle), $\theta_{\rm D}$ is the angle registration, β is the velocity of the electron in units of the speed of light and ε is the dielectric constant of the target material. For relativistic particles, $\beta\approx 1$, $\varepsilon = 1$, and take $n = 1$.

The photon distribution of the PXR at positions near the Bragg angle [photons per electron per steradian] is given by [6]

$$\frac{{\rm d}^2N}{{\rm d}\theta_x{\rm d}\theta_y} = \frac{\alpha}{4\pi}\frac{\omega}{c}\left[L_{\rm a}|\frac{\overrightarrow{n}\cdot\overrightarrow{\Omega}}{\overrightarrow{n}\cdot\overrightarrow{v}}|(1-{\rm e}^{-t/(L_{\rm a}|\overrightarrow{n}\cdot\overrightarrow{\Omega}|)})\right]\cdot$$
$$\chi^2{\rm e}^{-2W}\frac{\theta_x^2\cos^2 2\theta_{\rm B}+\theta_y^2}{\sin^2\theta_{\rm B}(\theta_x^2+\theta_y^2+\theta_{\rm ph}^2)^2},$$

here θ_x is the angular displacement from the Bragg condition in the diffraction plane, and θ_y is the angular displacement perpendicular to the diffraction plane, $\theta_{\rm B}$ is the Bragg angle, $\theta_{\rm ph}$ is approximately $1/\gamma$ (γ is the Lorentz factor), α is the fine structure constant, ω is the PXR angular frequency, c is the velocity, $L_{\rm a}$ is the absorption length of the PXR in the crystal, t is the crystal thickness, $\overrightarrow{v}$ is the unit normal to the velocity of electron, $\overrightarrow{\Omega}$ is unit normal to the velocity of PXR, χ is the Fourier expansion of the electric susceptibility, and $\overrightarrow{n}$ is the unit vector normal to the crystal surface.

The yield of the PXR increases with a larger absorption length ($L_{\rm a}$), because it allows more photons to escape the crystal. Therefore lower Z targets are chosen for the experiment, which at the same time leads to less unwanted Bremsstrahlung background. In general, to improve the PXR yield, a larger thickness of the targets would be desirable, but this would degrade the experiment by increasing the Bremsstrahlung, electron beam divergence, crystal heating and photon absorption [7, 8]. Si and LiF crystals with a thickness between 0.1 mm and 1 mm are attractive for the experiment. This article deals with a Si crystal with a thickness of 0.1 mm. Table 1 show the plane characteristics at 5.7475 keV.

Table 1. Crystal plane characteristics, assumed at 5.7475 keV.

crystal plane	$L_{\rm a}$/μm	$\chi(10^{-6})$	$d(10^{-10}{\rm m})$	heating/(mW/μA)
Si (111)	26.8314	2.271	3.14	195
Si (220)	26.8314	2.601	1.92	195

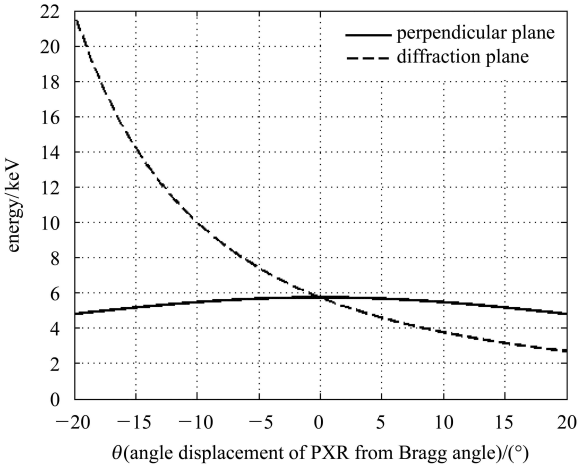

Fig. 1. Si (111) crystal (thickness is 100 μm): Energy distribution in the diffraction plane and perpendicular plane vs the direction displacement of the PXR from the Bragg angle. The Bragg angle is 20° and the electron energy is 10 MeV.

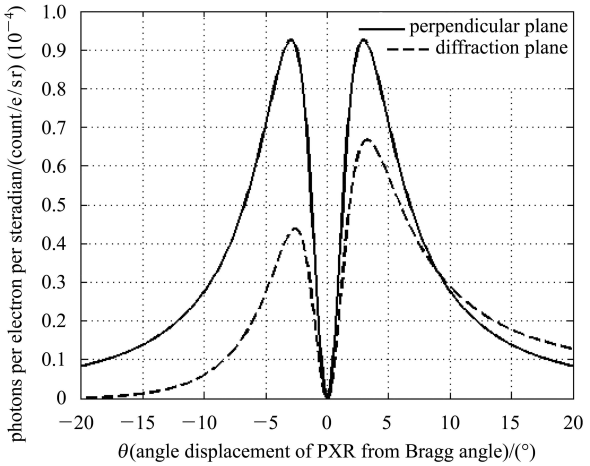

Fig. 2. Si (111) crystal (thickness is 100 μm): Photon distribution in the diffraction plane and perpendicular plane vs the direction displacement of the PXR from the Bragg angle. The Bragg angle is 20° and the electron energy is 10 MeV.

2.1 Energy distribution

Figure 1 shows the energy distribution of the PXR near the Bragg angle in the diffraction plane and in the perpendicular plane for an electron ($E = 10$ MeV) passing through a Si (111) crystal ($t = 100$ μm) with an angle of $20°(\theta_B = 20°)$.

2.2 Photon distribution

The photon distribution of the PXR near the Bragg angle [photons per electron per steradian] in the diffraction plane and the perpendicular plane is shown in Fig. 2.

2.3 PXR yield

The integral yield of PXR at Bragg angles within different solid angles are shown in the second row of the Table 2. But the maximal yield occurs at 0.9° displacement from the Bragg angle in the diffraction plane, and −2.8° displacement from Bragg angle in the perpendicular plane. The values are shown in the third row of Table 2.

Table 2. The photon yields at different solid angles.

solid angle/mrad	0.001	0.0028	0.01	0.1	1
integral yield (counts)	1.1335e-11	2.1486e-11	1.1335e-10	1.1333e-09	1.1329e-08
maximal integral yield (counts)	2.8983e-007	4.8306e-007	9.1652e-007	2.8982e-006	9.1635e-006
distance/m	5	3	1.518	0.5	0.1518
absorption coefficient	0.13682e-07	0.19129e-04	0.32617e-02	0.16354	0.56409
detected photons (counts)	3.9655e-15	9.2405e-12	2.9894e-09	4.7397e-07	5.1690e-06

The area of the detector is 25 mm^2 and the distances between the crystal and the detector are shown in the forth row of Table 2. Some photons are absorbed by air along the path. The absorption coefficients are shown in the fifth row of the Table 2. The counts of the photons detected by the detector are shown in the sixth row of Table 2.

2.4 PXR energy dispersion

As shown in Fig. 1, the space distribution ($\Delta\theta_x$ and $\Delta\theta_y$) results in a PXR energy dispersion, which will be increased by the electron beam divergence ($\Delta\theta_B$) and electron energy dispersion ($\Delta\beta$).

$$\Delta E = a\Delta\theta_x + b\Delta\theta_y + c\Delta\theta_B + d\Delta\beta.$$

For instance, consider a real electron beam ($\Delta\theta_B$=0, $\Delta\beta$=0) with 10 MeV pass through Si (111), then the energy of the PXR at a solid angle of 0.0028mrad is 5.4831 keV ± 19.9102 eV, and the energy dispersion is 0.73%.

3 Bremsstrahlung background

If an electron passes through a crystal, the X-ray background includes the dispersion of the electron, Bremsstrahlung, Transition radiation and Cerenkov radiation. In the X-ray wave band the electric susceptibility (χ_e) is negative [9] and the relative static permittivity (ε_r) is less than 1, such that Cerenkov radiation is impossible. The Transition radiation occurs mostly in the forword direction, peaking at an angle of the order of $1/\gamma$ relative to the particle's path. The X-ray background mostly is Bremsstrahlung.

The background calculation shown below was done with the software of FLUKA for the configuration just discussed.

3.1 Background at a solid angle of 0.01 mrad

If the detector is located at 1.518 m distance from the crystal, the total X-ray background amounts to 1.5114×10^{-8} photons and 4.1385677×10^{-9} photons between 0 keV to 110 keV. The photon distribution is shown in Fig. 3.

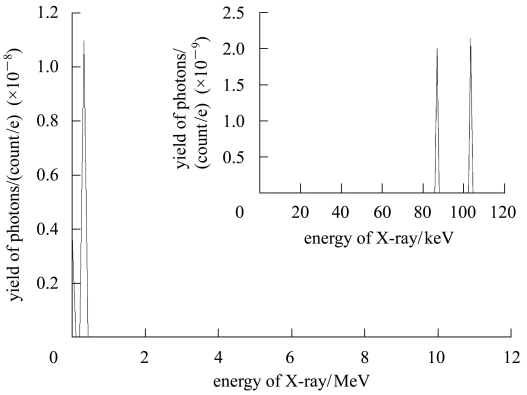

Fig. 3. Photon distribution of the Bremsstrahlung background at an angle of 0.01 mrad for the configuration described in the text. At the upper right corner the distribution between 0 keV and 110 keV at a Bragg angle of 20° is shown. The detector was placed 1.518 meters away from crystal.

3.2 Background at a solid angle of 0.0028 mrad

In this case the detector was located at 3m distance from crystal and a total X-ray background of 3.7187×10^{-9} photons and 1.5×10^{-9} photons between 0 keV to 110 keV have been obtained. The photon distribution is shown in Fig. 4.

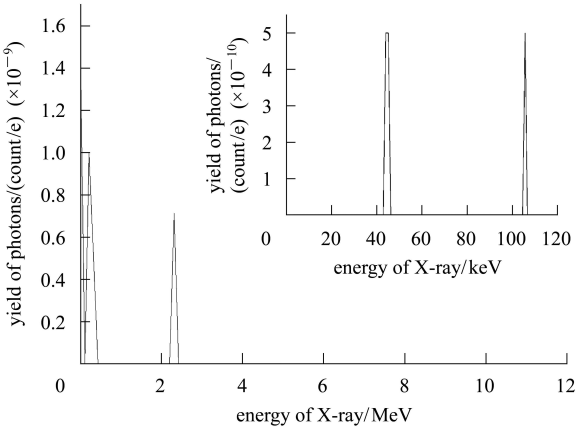

Fig. 4. Photons distribution of the Bremsstrahlung background at a solid angle of 0.0028 mradfor the configuration described in the text. In the upper right corner the distribution between 0 keV and 110 keV at the Bragg angle of 20° is shown. The detector was placed at 3 meters away from the crystal.

In addition the total background of the environment should be considered. It is produced mainly by the collisions of the electrons with the accelerating tube.

4 Design of the experiment

In the RPI (Rensselaer Polytechnic Institute) of USA one crystal is used in the PXR experiment [10] and in the Nihon University of Japan two crystals are used [11].

4.1 One crystal system

The electron beam coming from the output window is bent by 22.5° by a dipole magnet. Then it goes through two beam dumps for collimation and decreasing the radius of the beam. The detector, shielded by a lead sheath, is located at a distance of 1.57 m away from the Si (111) crystal at the Bragg angle, because at this distance the detected PXR photons are of the same order of magnitude as the Bremsstrahlung. It is easy to distinguish the PXR from the background. A schematic drawing of the experiment is shown in Fig. 5.

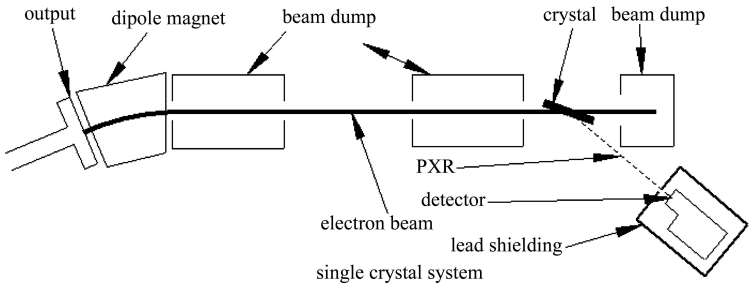

Fig. 5. The single crystal system. The first and second beam dumps with a hole in the middle (about 25 mm^2) are used for collimation and decrease the radius of the beam. The Bragg angle is 20°. The used crystal was Si (111).

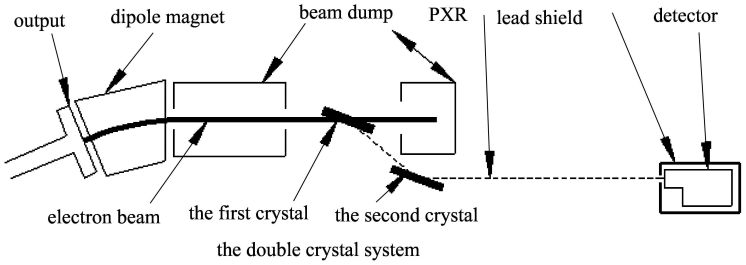

Fig. 6. The double crystal system. The PXR is distinguished form the background by the second crystal.

The current of the beam is calculated according to the following formula

$$\frac{\frac{1}{1\times10^{-6}}}{1.5114\times10^{-8}+2.9894\times10^{-9}}.$$

$$1.6\times10^{-19}=8.8\ (\mu\mathrm{A}).$$

The pulse current is 8.8 μA, and the radius of the beam is 2.8 mm, the same as of the detector. The beam current can be adjusted by a diaphragm of the klystron.

4.2 Double crystal system

The double crystal system is composed of two paralleled crystals. It is shown in Fig. 6.

The first crystal produces the PXR and the second one picks out the PXR from the background. The pulse current can reach up to tens mA through adjusting the distance between the detector and the crystal.

5 Summary

For a low energy electron beam based on the NCEL it is possible to produce and detect PXR through a single crystal or double crystals. Of course, in order to increase the luminosity of PXR, one should use a double crystal system, improve the pulse frequency and the magnitude of the electron beam current, locate the experiment in a vacuum environment, and use a no-energy-resolving detector, such as an ionization chamber.

References

1 Ter-Mikaelian M L. High Energy Electromagnetic Processes in Condensed Media. New York: Wiley-Interscience, 1972
2 Asseev A A, Gorin M Y. Nucl. Instrum. Methods. B, 1996, **119**: 210–214
3 Akimoto T, Tamura M, Ikeda J, Aoki Y, Fujita F, Sato K, Honma A, Sawamura T, Narita M, Imai K. NIM A, 2001, **459**: 78–86
4 Brenzinger K H, Herberg C, Limburg B, Backe H, Sambach S, Euteneuer H, Hagenbuck F, Hartmann H, Johann K, Kaiser K H, Kettig O, Kube G, Lauth W, Schope H, Walcher T. Z. Phys. A, 1997, **358**: 107–114
5 Wagner A R, Kuzentsov S I, Potylitsyn A P, Pazin S V, Uglov S R, Zabaev V N. Nucl. Instrum. Methods B, 2008, **266**: 3893–3897
6 Nitta H. Phys. Rev. E, 1995, **51**: 6305
7 Sones B, Danon Y, Block R C. Nucl. Instrum. Methods A, 2006, **560**: 589–597
8 Sones B, Danon Y, Block R. Nucl. Instrum. Methods B, 2007, **261**: 98–101
9 Kolpakov A V, Bushuev V A, Kuzmin R N. Usp. Fiz, Nauk, 1978, **126**: 479–513
10 Sones B, Danon Y, Block R C. Nucl. Instrum. Methods B, 2005, **227**: 22–31
11 Mori A, Hayakawa Y, Kidokoro A, Sato I, Tanaka T, Hayakawa K, Kobayashi K, Ohshima H. Nucl. Instrum. Methods B, 2006, **252**: 118–123